LU TP 18-29
September 2018

Performance of jet subtraction in pPb and PbPb collisions, without collectivity.

Sebastian Grabowski

Department of Astronomy and Theoretical Physics, Lund University

Bachelor thesis supervised by Leif Lönnblad

Abstract

We investigated the performance of basic jet subtraction, by the utilization of jet reconstruction generally used at the Large Hadron Collider (LHC). This was done by studying Z-bosons, in the dielectron decay channel, and the associated jet correlation in pp, pPb and PbPb collisions, using datasets generated by the Monte Carlo generator PYTHIA8. The PbPb collisions at $\sqrt{s_{NN}} = 2.76$ TeV and pPb collisions at $\sqrt{s_{NN}} = 5.012$ TeV were generated with the full simulated heavy-ion background by using the Angantyr model (PYTHIA), and compared to the results of pp collisions with a corresponding collision energy. The way the Angantyr model works is by essentially stacking individual nucleon-nucleon sub-collisions on top of each other and hadronize them together, allowing us to study only the microscopic interactions without any assumptions of a thermalized medium or collective interaction. The measurements of Z+leading-jet from these collisions are presented as a function of the transverse momentum balance between Z^0 and the jet, the azimuthal angular and the pseudorapidity separation between the Z^0 and the jet, and the jet profile. These measurements are presented as a function of collision centrality. The results of the investigation suggests that the jet subtraction performs considerably well correcting the transverse momenta of the jet for peripheral PbPb collisions and pPb events, but the shape of the jets remain strongly damped in the underlying event of central PbPb collisions.

Popular Scientific Summary: Recreation of Big Bang

When head-on collisions between massive lead ions are performed at the Large Hadron Collider, there are hundreds of collisions happening at once creating tens of thousands of particles, at energies of a few trillion electronvolts. This firework of particles forms for a brief moment a tiny "big bang" so hot that everything inside it "melts" into a so-called *quark-gluon plasma*, or QGP for short.

The quark-gluon plasma is a system so incredibly hot and dense that quarks and gluons, the building blocks of all ordinary matter, are no longer bound to their primary *hadron*, but can freely interact with e.g. quarks from other hadrons. At this brief moment, we have recreated the conditions similar to those that exist in the very early moments of the universe.

As this ultra hot fireball expands and cools down immediately afterwards, the individual quarks and gluons recombine into their natural bound states, such as protons and neutrons and other less familiar and unstable hadrons. These particles are then dispersed in all directions and detected with a gigantic detector system. The information carried by these particles is very important to our advancement of knowledge of *quantum chromodynamics*, which is the theory describing the nature of quarks and gluons. Together with the electrons they form the building blocks of everything we see around us.

In order to make any sense of the circus of particles registered by the detectors, we need a physical theory and models, that are able to explain the outcome and what has happened. These collisions are, however, normally described with statistical models, which deals with averaged properties, such as pressure, density and temperature. With this in mind, a group of people at the Lund University has developed a new event generator model, which will simulate heavy-ion collisions in great detail, down to the individual quarks and gluons, in order to separate effects of different origin.

My role is to investigate the performance of basic methods of analysing heavy-ion collisions, simulated by the new event generator. These methods rely on an indirect observables that are sensitive to the effects of the QGP. The observable is a spray of particles, a so called jet, that passes through the plasma. At very rare occasions, the primary collision between a combination of two quarks/gluons from each lead ion, produces a very energetic electron-positron pair, that will pass the plasma unchanged. Together with this, we get a corresponding recoil of particles in the opposite direction of equal magnitude, a "hard jet", that will interact strongly with the surrounding quarks and gluons in the quark-gluon plasma. This type of hard scattering is extremely instructive, as it can provide information on the jet modification that occurred in the plasma, thus revealing properties of the quark-gluon plasma.

This new event generator will serve as a very powerful tool and may help future studies, as it will contribute to the understanding of the quark-gluon plasma and the forces behind the most elementary particles. All in all, it will give us one more piece of the puzzle, that is to understand the origin of matter and the beginning of our universe.

Contents

List of Figures

List of Tables

1 Introduction

At the Large Hadron Collider (LHC) at CERN, scientists are studying collisions of both the smallest atomic nucleus, single protons, as well as the heavy-ion of lead, consisting of 208 protons and neutrons. Our methods of calculating and modelling the final states for single proton collisions are well described by so-called *event generators*, giving us a detailed description of the hundreds of particles produced in such an event. However, despite the major success in recreating these events in simulations, our theoretical models of heavy-ion collisions leave a great deal to be desired. This is due to a rather poor generalized implementation in existing event generators of effects such as jet quenching, elliptic flow and quarkonium suppression ascribed to the formation of a so-called *Quark-Gluon Plasma* (QGP).

The available event generators for simulating the heavy-ion collisions, which produces tens of thousands of final state particles, normally utilize hydrodynamical models (such as EPOS-LHC [1], AMPT [2]), i.e. statistical models that mainly characterizes averaged properties (pressure, density, temperature etc.), based on the assumption of a expanding thermalized medium. These hydrodynamical models focus on describing collective effects signalling the formation of a QGP. With this in mind, a new event generator model has been developed at Lund University called Angantyr [3], which in contrast focuses on the interaction between individual particles and to a large extent ignores collective effects (without the assumption of a thermalized medium). One may note that this is not unique for Angantyr, e.g. HIJING [4] is built on a similar starting point. The Angantyr model will give us a highly useful theoretical tool for studying the non-collective background in heavy-ion collisions to sensitively probe the thermodynamical properties of the produced medium.

To study the quark-gluon plasma, we need to probe the early stages of the dense system's evolution created in heavy-ion collisions, which lasts for an order of a few fm/c in transverse direction [5]. Since experimentally made observations are mainly on the final state particles, we need probes that are already in existence at the earliest of stages and that are sensitive to the properties of the medium. Prime candidates for studying the QGP are the so-called *hard processes*. They are characterized by the back-to-back scattering of two partons with large momentum transfer, originating from the initial crossing of the heavy-ions. An example of these probes are *jets*, collimated sprays of particles produced from fragmentation of the original partons that participated in the hard scattering. The production time-scale of these processes is $\tau \approx 1/p_T \lesssim 0.1$ fm/c [6], allowing them to act as "tomographic" probes for studying the medium.

It was early on proposed by Bjorken [7] that energetic partons traversing the quark-gluon plasma would lose energy to the medium, scattering off any encountered in-medium particles. This would yield in a high-p_T hadron suppression. The first observation of this phenomenon, dubbed *jet quenching*, was observed at BNL (RHIC) from the $\sqrt{s_{NN}}$ =130 GeV Gold central collisions STAR experiment [8]. Another observable suggested by Bjorken

(in the same work) was the dijet[1] asymmetry in the transverse momentum (p_T). This was noticed in the $\sqrt{s_{NN}}$ =200 GeV Gold collision [9] and later confirmed with the ALTAS detector at the LHC [10], showing p_T-imbalance between two reconstructed jets originating near the edge of the overlapping nuclei (i.e. at the periphery of the collision), resulting from different amounts of energy loss. The advantage of using dijet-events as QGP probes is that they have a large cross section. However, both partons will suffer energy loss.

A more instructive, however rarer in comparison with purely QCD processes, variant of hard scattering involves the production of an electroweak boson (γ, W, Z). These bosons, with high transverse momenta, will remain unmodified by final-state interactions [11, 12] and therefore retain the kinematic information of the scattered parton, which can be used to unbiasedly characterize the in-medium parton energy loss. In the case of Z^0 production, the Z^0 can be produced with an associated parton, $q\bar{q} \rightarrow Z^0 g$ and $q(/\bar{q})g \rightarrow Z^0 q(/\bar{q})$. In turn, we want the Z-boson to decays into leptons, which are also unaffected by QCD and the dilepton signatures are fairly easy to identify. The high transverse momentum of the boson will in turn produce a partonic recoil of the same magnitude, in the diametrically opposite direction in the transverse plane, an associated *hard jet*. In heavy-ion collisions, the high-p_T jet will experience in-medium energy loss while propagating the medium [13, 10, 8]. This modified jet can provide important information on the properties of the medium and interaction processes.

Jet reconstruction in heavy-ion experiments is problematic because of the overwhelming background of soft or moderately hard particles accompanying the production of hard partons and/or vector bosons, defined as *underlying event* (UE). With this in mind, the method for jet reconstruction used here is the anti-k_T algorithm, chosen due to its jet boundary being resilient to the effects of soft particle fluctuations in the background. Furthermore, the underlying events also produce a significant alteration of the reconstructed jet energy, and are thus requiring jet subtraction. This is done by calculating the energy density corresponding to the underlying event.

There are several different observables for jet-modifications in the QCD medium. For instance, one can expect significant changes to the particle distributions inside the jet, the so-called jet profile, as these particles will scatter off the various constituents that it encounters. There are observations of suppression of heavy quarkonia, dijet asymmetry and p_T imbalance between bosons and the associated jets. In this thesis, we will restrict ourselves to observations of the jet profile, p_T imbalance and correlations in the pseudorapidity and azimuthal angle between the reconstructed Z-boson and jet.

This thesis is set up as follows. Chapter 2 contains a theoretical overview of heavy-ion collisions, relating concepts and methods of measuring properties of the quark-gluon plasma. In chapter 3, the focus lies on the jets. Here we will go through the background of jets (i.e. their definition, both the theoretical and the experimental one), followed by how jets are found and finishing with the major effects found in heavy collisions on jets. In chapter 4, a theoretical overview will be provided on the Monte Carlo generator with a

[1]Dijets are the produced from a hard scattering process which resulted in two fragmented partons with the transverse energies in opposite hemispheres.

short description of the heavy-ion model, Angantyr (Chapter 4.1.1). The following chapter, Chapter 5, will describe the simulation part of this thesis, together with the analysis methods, event selection, jet reconstruction and background analysis. In this chapter we will go through the methods used in jet subtraction and provide a slight modification. The results of Z+jet analysis and the corresponding performance of the background subtraction are provided in chapter 6. A discussion of the mentioned results and analysis methods concerning the background subtraction are provided in chapter 7, followed by a review and conclusions in chapter 8.

2 Study of the Quark-Gluon Plasma

The widely accepted underlying theory of the strong interaction is the so-called quantum chromodynamics (QCD) one. This theory is described by a non-Abelian SU(3) gauge theory, first proposed by M. Gell-Mann and Y. Ne'eman [14, 15], which possesses features leading to phenomena such as colour confinement (at low-energy scales) and asymptotic freedom (at high-energy scales), as can be deduced from figure 1. The colour confinement, which states that quarks and gluons can only exist in bound states within hadrons, occurs in the low-energy scale regime where $\alpha_s(Q) \sim \mathcal{O}(1)$. This magnitude of coupling strength prohibits the use of perturbation theory for calculating the higher-order Feynman diagrams. Nevertheless, this problem can be solved with *lattice QCD*: computational calculus for solving QCD theory numerically, performed on a discrete lattice of points in space and time. At the typical high energy scale (or conversely at small length scale) achievable in modern high-energy collider experiments ($Q > 100$ GeV), the strength of the QCD coupling decreases substantially, sufficiently for use of perturbation theory, with higher-order corrections. This reduction of α_s indicates that quarks and gluons could essentially behave as quasi-free particles inside a hadron at high energy scales. This behaviour is known as *asymptotic freedom*. It was suggested that this property of QCD, of having asymptotic freedom (at high energy scales and/or short length scales) and colour confinement (at low energy scales and/or long length scales), could contain a phase transition between high and low temperatures and/or baryon densities that would be accessible to experimental investigation. The first detailed examination of this proposed phase of quark-gluon-deconfinement, named the quark-gluon plasma (QGP), was conducted by Shuryak in 1980 [16].

The only way of observing the QCD matter in collision experiments is by indirect means: detecting observables predicted to be sensitive to the creation of a quark-gluon plasma. This topic will be touched upon in the following section.

2.1 Experimental measurement of QGP properties

The experimentally most reliable way of achieving the necessary high temperatures and energy densities for the QGP phase transition to occur (predicted from lattice QCD [18], in order to account for non-perturbative effects) is by colliding heavy-ions at ultra-relativistic

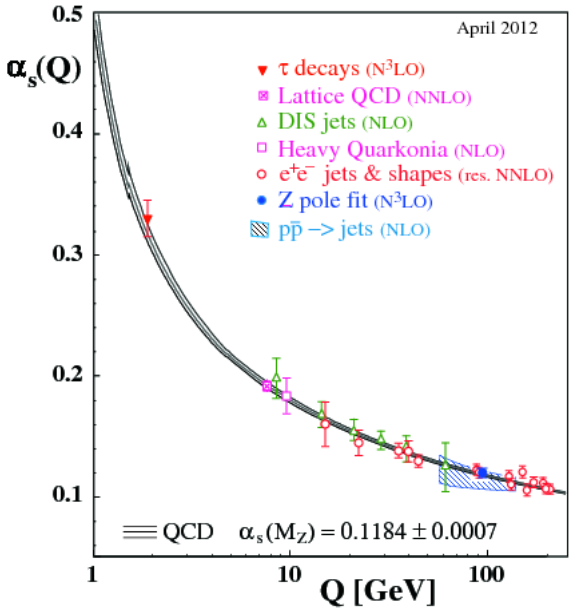

Figure 1: Summary of measurements of α_s, which shows that the coupling constant have a dependence on the considered interaction energy scale, Q. For low energies, α_s increases asymptotically, which leads to confinement. For large energy scales, however, α_s decreases and approaches 0, which leads to asymptotic freedom. The figure is taken from [17].

energies. The results obtained from the analysis of these collisions are frequently compared with reference data (such as pp and pPb collisions), in order to identify any modification[2] caused by initial- or final-state effects. Consequently, the baseline for heavy-ion collisions can be drawn from collisions where the physics processes are well described and where it is believed that no QGP is formed, thus providing direct information on the underlying QCD medium. However, there exists processes that can mimic some of the effects of the deconfined plasma (one of them is explored in [19]). The strategy for distinguishing these effects from QGP effects is by studying smaller collision systems, such as proton-proton[3] and proton-nucleus[4] collisions.

There exists quite a few available experimental observables that are expected to provide information on the properties and evolutions of the QCD matter (some of these are mentioned in section 1 of [21] and section 1.5 of [22]). Typically, these observables can be described as *the modifications of specific particle properties caused by interactions with the QGP*. For instance, quarkonium suppression (disappearance of quarkonia states, e.g. J/Ψ [23]) due to colour screening, collective flow of the medium, and high-p_T hadron suppression due to medium-induced energy loss of the initial partons. In this study, we will focus our attention on the latter, and more specifically on the jet quenching phenomena and the experimental observable of jet quenching in Z^0+jet production.

[2]Heavy-ion collisions are not only a superposition of independent proton-proton collisions, but give rise to a full set of new phenomena, such as secondary collisions of quarks and geometric dependences.

[3]The pp collisions are used as a baseline for "ordinary" QCD phenomena.

[4]The pA collisions were introduced to account for the initial wave function (nuclear PDFs) and its fluctuation of the colliding nuclei. This would enable us to disentangle these nuclear effects originating from the initial state structure of the collision (with effects such as shadowing and saturation) from the final-state effects, thought to be related to the medium [20].

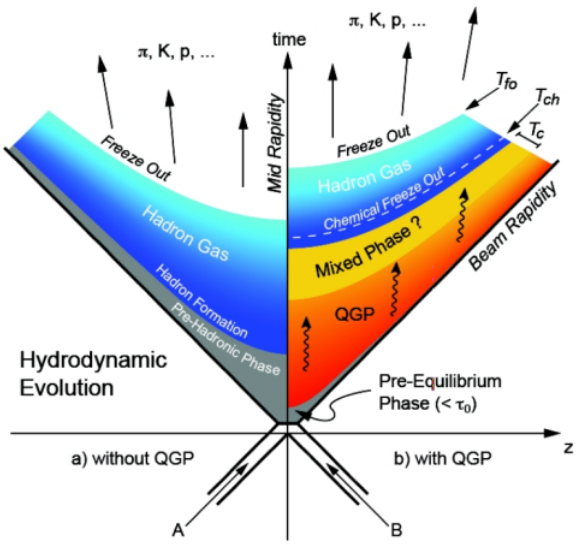

Figure 2: This figure illustrates the evolution of a central heavy ion collision in space and time. The time axis separates two collision scenarios: one were the the critical temperature and energy density is not achieved for QGP formation (left) and the another were the conditions are achieved, producing QGP (right). The variables denoted on the figure are as follows: the critical temperature T_c, the freeze-out temperature T_{fo} and chemical freeze-out temperature T_{ch}. The figure is taken from [24].

2.2 Collisions of Nuclei

When colliding ultrarelativistic heavy-ions, one can separate the evolution of this collision into several stages, as illustrated in figure 2. In the case were the critical temperature and critical volume for QGP formation are not reached, the system will expand according to hydrodynamical evolution (left half of figure 2) without deconfinement occurring and will proceed directly with the hadronization process. In the case where the conditions are reached, the collision of the heavily Lorentz-contracted (disk-shaped) nuclei induces a stage often called the *pre-equilibrium* stage. At this stage, the hard processes will begin to take place, at similar times as the creation of a QGP. When this system reaches thermal equilibrium, the QGP matter is produced. This system will then expand due to the inner pressure, in correlation with decreasing temperature, leading to gradual hadronization of the partons spreading with the speed of sound, the *mixed phase*. The geometry of the expansion[5] depends on the initial geometry of the collision, which will be discussed in section 2.2.1. The hadronization of quarks and gluons in the medium results in *fragmentation* of high p_T partons into lower p_T hadrons (at high energies) and *coalescence* of low p_T partons, combining them into higher p_T hadrons (at low energies). When the distances between hadrons rule out elastic rescattering (hadrons decouple), we enter the *chemical* and *thermal freeze-out* stage were the chemical composition and kinematics of the system becomes fixed.

2.2.1 Collision Geometry

Since the colliding heavy-ions are rather extensive objects compared to individual colliding protons, the collision system will differ remarkably depending on how "central" the collision

[5]The observable connected to the geometry expansion is collective flow. This results from the collective behaviour of thermalized medium and can manifest itself as radial flow and elliptic flow.

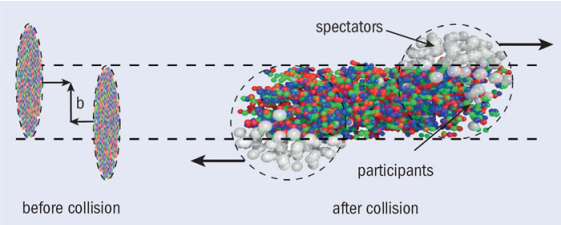

Figure 3: Illustration of the concept of centrality and the related impact parameter b. Participants refers to the nucleons taking part in the interaction, while spectators are the non-interacting nucleons. The figure is taken from [25].

was[6]. In order to distinguish the initial geometry of the collisions, one can introduce an *impact parameter*, b, which is defined as the transverse distance between the center of the colliding nuclei, as can be seen in figure 3. However, the impact parameter is not a physical observable. From the experimental point of view, when presenting data from heavy-ion collisions, one typically categorized them by *centrality*, an observable coupled to the activity (often in the forward/backward direction) of the collision. Centrality is defined as the percentile of events with largest number number of produced particles, registered by detectors. As can be deduced from figure 3, this centrality observable should have a monotonic relationship with the impact parameter, b: the larger number of , *participants* (i.e. nucleons undergoing at least one collisions), the smaller the impact parameter (greater the overlap area of the colliding heavy-ions). In turn, the number of participants is assumed to be directly coupled to the activity.

3 Jets

Hadronic jets are defined as collimated hadrons resulting from the fragmentation of a sufficiently energetic outgoing parton, originating from an initial hard scattering process, as mentioned in section 2.2. In practise, jets are defined from experimental observables (i.e. particle 4-momenta) and are therefore algorithm-dependent, meaning that there is no unique or correct way to group these hadrons. These algorithms generally work by clustering the final-state particles that are close in momentum-space (i.e. particles that go towards the same direction), in a rough attempt to reconstruct the kinematics of scattered partons.

The reason why hard jets are so useful for studying QCD matter (such as QGP) is due to their properties: they directly couple to the QCD degrees of freedom, due to their partonic origin; their short production time-scale of $\tau \approx 1/p_T \lesssim 0.1$ fm/c, allowing for both traversing and being modified by the QCD medium; they have theoretically predictable cross sections (perturbative QCD).

[6]As an example, the centrality have a huge influence on the collective flow. A peripheral collision has a almond-shaped overlap and resulting in a different pressure gradients in different directions from centre to border of the overlap region, creating a direction dependent flow.

3.1 Evolution of Jets

The jet evolution and the analysis can be summarised into 6 steps:

1. Initial state radiation: Before the actual hard-scattering of partons within the incoming colliding hadrons, there is a possibility for initial state radiation of these partons, resulting in modifications of the energy, the topology and the multiplicity of the outgoing particles.

2. Hard-scattering and final stage radiation: The hard-scattering process are processes where the scattered particles have high momentum transfer. After these have occurred, the scattered partons may produce *final state radiation*, which is similar to the initial state radiation. At the scale of final state radiation, perturbative process continue to produce emissions, resulting in a cascade of partons moving approximately in the direction of the original parton.

3. Fragmentation and hadronization: The evolution of the parton cascades continues until the energy scale (or virtuality), q^2, falls from the hard process scale to the cascade cut-off scale, where we can no longer rely on perturbative calculations ($\alpha_s(q^2)$ becomes too large) as we enter the low momentum transfer and long-distance regime. At this point, the non-perturbative hadronization mechanism takes effect. The type of model used in theoretical calculations for the fragmentation of the scattered partons depends on the used Monte Carlo generator. The PYTHIA8 generator uses the Lund string model [26, 27], where the word "string" originates from the narrow tubelike shape of strong colour fields, due to gluon self-interactions. The basic idea is that the process of transforming a partonic final state (e.g. two partons in a $q\bar{q}$ system moving apart from each other) to a hadronic one, can be viewed as a continuing processes of longitudinal stretching of the string fields (separation of partons) and string break-ups[7] (creation of a quark and anti-quark pair) into smaller segments until only on-mass-shell hadrons remain. This is illustrated in figure 4.

4. Particle decay: in this stage of the jet evolution, the internal particle interaction have ceased, but the short lived unstable particles may decay into a series of final state particles.

5. Registration by detector and detector effects (which is left out in this thesis): The final jets' constituents are then registered by the detector.

6. Jet reconstruction: The registered particle information is then analysed by jet reconstruction algorithms, which produces the final observable jets.

   Particles that did not originate from the hard scattering are referred to as the underlying event. The underlying event is a convolution of several contributions from

[7] The breakage occurs naturally, depending on whether the string invariant mass is greater than an on-shell hadron.

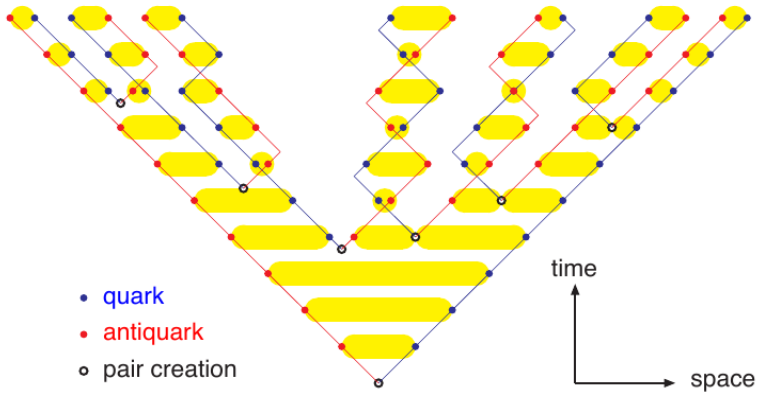

Figure 4: This figure illustrates the main idea of the Lund String Model, a theoretical model on fragmentation. The yellow thick lines represents the colour strings. The Fragmentation starts in the middle and spreads outwards. The colour string stretches and breaks into 2 colour singlet strings, i.e. creating a quark-antiquark pair. The figure is taken from [28].

multiple parton interaction and beam remnants and their interactions. In heavy-ion collisions, these interactions can induce energy loss of the partons originating from the hard scattering, referred to as jet quenching. Most commonly, however, the underlying event tends to obscure the signal of interest and may lead to corrections of the reconstructed jet energy that can be needed to be corrected, with jet subtraction methods.

3.1.1 Experiment

In practice, jets differ substantially from the theoretical picture given above. This is because of the fact that only final state particles are available for observation, implying that the information on original parton was lost during the hadronization phase of the collision. So, experimentally speaking, jets are a collimated spray of particles and energy. In the next section, Section 3.2, we will discuss the experimental definition of jets and how jets are experimentally found. In addition to this definition, there will be new uncertainties introduced by the presence of the underlying event, that will require an energy correction on the jets. The discussion on the underlying event is held in section 3.3 and the subtraction of the underlying event is described in section 5.4.2.

3.2 Definition of Jets

The way of finding jets, in practice, boils down to a clear and usable jet definition. The general accepted "recipe" for jet finding is in accordance to the Les Houches convention described in [29]: a 'jet definition' should include the jet algorithm used in reconstruction, its parameters (in our case, the radius R) and the recombination scheme.

In the following sections, we will only focus on presenting the specific type of jet definition criteria that were used in this thesis.

3.2.1 Algorithms

Before presenting the used jet algorithm, let's define the space coordinate system. A frequently used coordinate system in accelerator physics is the cylindrical coordinate system (z, ϕ, η) (due to the cylindrical geometry of experiments), where the beam axis is associated with the z-axis and ϕ is the azimuthal angle. However, instead of using θ as the polar angle, it is often given in terms of the pseudorapidity,

$$\eta \equiv -\ln\left(\tan\frac{\theta}{2}\right). \tag{3.1}$$

The pseudorapidity is a massless approximation of the rapidity,[8]

$$y \equiv \frac{1}{2}\ln\left(\frac{E+p_L}{E-p_L}\right) \xrightarrow[E\to p]{} \frac{1}{2}\ln\left(\frac{p+p_L}{p-p_L}\right) = \frac{1}{2}\ln\left(\frac{1+\cos\theta}{1-\cos\theta}\right) = -\ln\left(\tan\frac{\theta}{2}\right) \equiv \eta, \tag{3.2}$$

where y is rapidity, $E = \sqrt{p^2+m^2}$ and $p_L = |\mathbf{p}|\cos\theta$. The key reason for using rapidity, respectively pseudorapidity, is that the rapidity intervals are invariant with respect to Lorentz boosts along the beam axis[9].

Now that the geometry of the system has been established, we can introduce the concept of jet algorithms, or more specifically: the sequential recombination "anti-k_T" algorithm, which was used. This type of algorithm utilises *hierarchical clustering*, which is a iterative procedure of recombining the pairs of particles that are closest in some distance measure until a criterion is reached. The calculated distance of a particle pair, d_{ij}, (involved in the "generalized" k_T algorithm) is defined as

$$d_{ij} = \min\left(p_{T,i}^{2p}, p_{T,j}^{2p}\right)\frac{\Delta R_{ij}^2}{R^2} = \min\left(p_{T,i}^{2p}, p_{T,j}^{2p}\right)\frac{\Delta y_{ij}^2 + \Delta\phi_{ij}^2}{R^2} \tag{3.3}$$

where $p_{T,i}$ is the transverse momentum of particle i with respect to the beam (z-axis) direction, ΔR_{ij} is the distance between particle i and j in (y, ϕ), and R is the so called jet radius (see section 3.2.2). The different k_t algorithms are separated by the choice of p: the original k_t-algorithm ($p = 1 \implies$ merges low-p_T particles first[10]), Cambridge/Aachen ($p = 0 \implies$ geometrically the closest) and anti-k_t ($p = -1 \implies$ merges high-p_T particles first). Another distance measure in the k_T algorithm is the distance between particle i and the beam,

$$d_{iB} = p_{T,i}^{2p}. \tag{3.4}$$

[8] A rapidity measurement requires both the energy and the total momentum, which is often difficult to get a precise measurement of, especially at high y values near the beam axis. This makes pseudorapidity much easier to measure.

[9] This is useful as the longitudinal momenta of the colliding partons inside the nuclei are a priori unknown in each individual collision, and the resulting relative motion can be understood as a boost of the constituent system with respect to the lab or beam system.

[10] This characteristic is useful in determination of background, as it merges the contribution which mostly originates from soft processes. This forms a boundary of the jet area that is heavily affected by soft radiation of the underlying event.

These two distances are then compared, in the search of the smallest one. If d_{ij} is the smaller one, one recombines these two particle into one "pseudojet", using a *recombination scheme* (see section 3.2.3). If d_{iB} is smaller, then i is removed from the of list of particles/pseudojets, adding it to the list of final "inclusive" jets. This procedure continues until the list of particles/pseudojets is empty. The resulting list of final jets may contain jets of a single particle, but each particle is associated to only one final jet. These jet can later on undergo selection and rejection in the analysis, depending on the given criteria (e.g. minimum transverse momentum cut).

3.2.2 The R-Parameter

In the already defined space of rapidity and azimuthal angle, the radius parameter R (also called the resolution parameter) serves as a maximal distance between the jet axis and its components, i.e. the jet radius. It is important to know that the choice of value for this parameter require some forethought: high values ensure that the whole jet is contained within the given area, however, at the expense of increasing contribution from other sources.

3.2.3 Recombination Scheme

The recombination scheme describes the way in which individual particles are merged. The recombination scheme chosen in this thesis was the *energy scheme*, were the four-momentum of a jet is defined as the sums of the four-momentum of its constituents. This recombination scheme is advocated as a standard and used by the LHC experiments.

3.3 Underlying Event

The Underlying event (UE) is everything that did not originate from the initial hard-scattering or the hard process of interest: beam-beam remnants (partons that did not interact, *spectators*) and multiple parton interactions (MPI) (scattering of multiple partons of the same hadron). This is illustrated in figure 5 as any colour that is not red (hard-scattering) or blue (incoming particles). The contribution of the UE increases further with higher energy scales at small longitudinal momentum fractions x, as the occurrence of a MPI process depends strongly on the density of partons inside the colliding nucleons. This parton density increases with higher energy scales and at small x, leading to increased probability of additional processes in the UE.

In AA collisions, the cumulative effect of UE processes is drastically more abundant than in proton-proton collisions, due to the numerous amount of participating nucleons. This is challenging because the jet algorithm will sweep up any soft particle, and likely swamp the jet by the underlying event, making jet reconstruction difficult, requiring it to be studied on a event-by-event basis. The discussion on a simple procedure of handling the UE can be found in section 5.4.2.

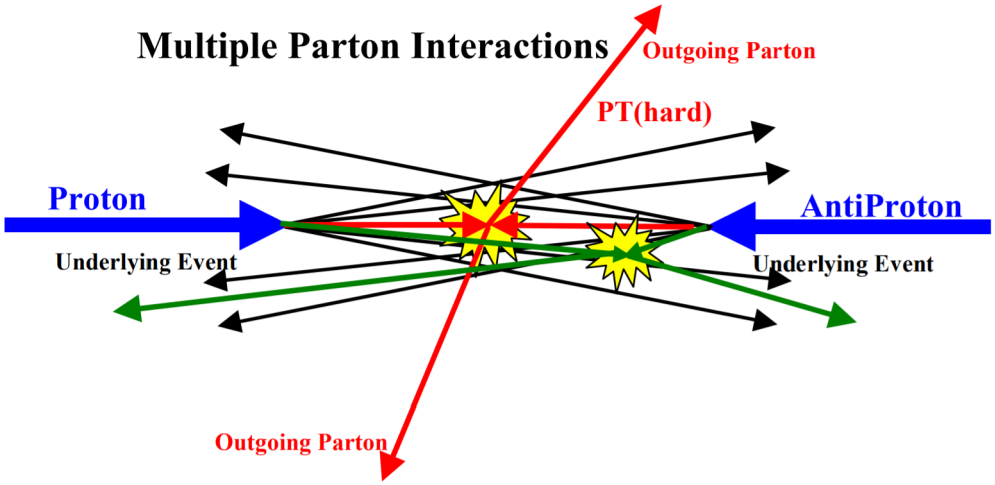

Figure 5: This figure illustrates the underlying event in proton-antiproton (blue arrows) collisions, with multi-parton interactions (MPI) (green arrows). In addition to the 2-to-2 hard-scattering (red arrow) with transverse momentum, "PT(hard)", there is a probability for a second interaction between other two partons. The figure is taken from [30].

4 Simulation Programs

4.1 The Monte Carlo event generator

Experimental data is, by itself, essentially useless without physical theories and models able to explain the outcome and what has happened. The opposite is also true, that theoretical predictions are meaningless without experiments checking the validity of them and tuning the parameters. An essential tool, in collider experiments, to bridge the gap between experimental data and theoretical predictions is the *Monte Carlo event generators*. Monte Carlo event generators are large computer program libraries filled with theoretical models used for simulating individual particle collisions (called events) in order to describe, as accurately as possible, the physics behind the observed experimental characteristics. Together with *detector simulation programs* (such as GEANT [31]), they are indispensable for data analysis, providing a realistic estimate of the detector response to collision events, and in the planning of current and future experiments (along with devising analysis strategies for these experiments), where they are used to estimate signals and backgrounds in high-energy processes (what type of events to expect and their production rate) and optimizing the detector performance. In this allows us to do a physics analysis which may provide new information about the fundamental particles and further our knowledge of particle physics.

This thesis, we only utilize the PYTHIA8 Monte Carlo event generator. The heavy-ion model used to generate the heavy-ion background will be given a short overview in the follow section, Section 4.1.1.

4.1.1 Angantyr - The heavy-ion model

Version 8.230 of PYTHIA comes with a newly included model, called Angantyr [3], for simulating heavy-ion collisions by realistically combining several nucleon-nucleon (NN) sub-collisions and hadronizing each sub-collision separately, inspired by the Fritiof model [32] with improvements described in [33].

The rough idea of the methodology for generating final states goes as follows [34]: In both of the colliding nuclei (labelled as "projectile" and "target"), each nucleon is viewed as an individually fluctuating semi-transparent disk. The nuclei consists of nucleons distributed according to a Woods-Saxon potential. The radii, transparency and fluctuation probabilities are then adjusted to fit the non-diffractive ($N + N \rightarrow X$) nucleon-nucleon cross section, as well as the elastic, single- ($N + N \rightarrow X + N$) and double- diffractive cross sections. This division of inelastic sub-collisions is achieved by using a model, inspired Strikman et al. [35]. Each possible sub-collision is generated by PYTHIA as a NN collision and treated (in the manner described above and) separately in terms of colour reconnection and hadronization with the Lund string model (no cross talk between each sub-collision). Note that each projectile nucleon may interact with several target nucleons and vice versa. The primary and secondary absorptive interaction are distinguished, as a nucleon that has already interacted before is arguably different, and so the secondary are treated in a special way [3].

An important detail of the current version of the used Angantyr model is that it is missing collectivity in hadron collisions[11]. This basically means that there is nothing in the model that can reproduce the effects of the quark-gluon plasma, mentioned in section 2. This includes, among other things, jet quenching and the long range azimuthal correlations, which forms a so called ridge in the angular distribution of particles. This will allow us to study the effects of individual hadronization in the absence of collective effects. The model can therefore serve as a tool to distinguish and understand the influence of other non-collective mechanisms on observables designed to be sensitive to collective behaviour. Examples of this is that jet reconstruction is highly influenced by the high multiplicity and energy of the underlying event in jet quenching. Modifications of the jet shape, inner structure and hadron distribution attributed to the QCD medium, may be the results of region-to-region fluctuations of the UE caused by the initial state of the collision. The underlying event in jet quenching is explored in ref [37]. Other mechanisms that can explain collective behaviour are discussed in ref. [19]: strangeness enhancement can be explained as overlapping strings (Lund string model) causing a superposition-like response called "ropes" as shown in pp [38, 39], pPb and PbPb [40] events. The formation of a "ridge" caused by elliptic flow-like effect in pp can be obtained from increased energy density resulting in a transverse expansion [41, 42].

[11] Currently, there exists a model that can qualitatively reproduce soft features of Quark Gluon Plasma (in small system) [36], but is not implemented in the used version of Angantyr.

5 Monte Carlo Simulation and Analysis Procedure

The Monte Carlo (MC) event generator used for this simulation is PYTHIA8 (version 8.230, released in October 2017), with FastJet version 3.3.0. performing the event analysis. The analysis is performed by using generated events for lead (PbPb) collisions at $\sqrt{s_{NN}} = 2.76$ TeV and proton-lead (pPb) collisions at $\sqrt{s_{NN}} = 5.012$ TeV. For the pPb event, the beam energies were 4 TeV for protons and 1.58 TeV per nucleon for lead nuclei. For comparison, proton-proton (pp) collisions are generated with corresponding collision energies and with and without the MPI setting.

The center-of-mass energy for a nucleon-nucleon (NN) collision, when two beams of nuclei A and B, with charge Z_A, Z_B and atomic numbers A_A, A_B resp., is given by [43]

$$\sqrt{s_{NN}} = \sqrt{\frac{Z_A Z_B}{A_A A_B}}\sqrt{s}, \tag{5.5}$$

if they are accelerated with the same magnetic rigidity.

A summary of all requirements on the selected events are presented in table 2 and a summary of the parameters used for the event set-up run in PYTHIA is found in table 3.

5.1 Simulation Time

The heavy-ion collisions are computationally quite processing intensive and generating a single event (with the used setting) takes about one second. In order to get reasonable statistics, we used Lunarc's Aurora computing cluster, allowing us to generate large amount of events with a parallel, distributed PYTHIA simulation, on this cluster. With the given cuts for the events (summarised in table 2), the acceptance rate for the event selection is very low, $\sim 8\%$ for pp events, $\sim 6\%$ for pPb events and $\sim 1\%$ for PbPb events.

Cuts:	**pp (no MPI)**	**pp**	**pPb**	**PbPb**
$p_T^{e^+}, p_T^{e^-} > 20$ GeV/c	25%	24%	24%	24%
$\lvert\eta^{e^-}\rvert, \lvert\eta^{e^+}\rvert < 1.1$	58%	58%	58%	54%
$p_T^{\text{jet}} > 30$ GeV/c	8%	8%	8%	3%
$\sqrt{(\phi^{\text{jet}} - \phi^{\text{Z}})^2 + (\eta^{\text{jet}} - \eta^{\text{Z}})^2} > 0.52$	0.0%	0.0%	0.0%	11%
$\lvert\phi^{\text{jet}} - \phi^{\text{Z}}\rvert > 2.6$	2%	3%	7%	6%
% of passed events	5%	8%	6%	1%

Table 1: The percentage of Z+jet events removed by a given cut in preceding order.

5.2 Event Selection

The selection requirement of the generated events for the analysis are events containing Z+jet (see the summary of requirements in table 2): production of a single Z^0 (decaying to

a dielectron pair) in combination with a parton, produced by the hard scattering process[12]. The selected decay products of the Z-boson candidate are required to be within the fiducial region of $p_T^{e^+e^-} > 20$ GeV/c and pseudorapidity $|\eta^{e^+e^-}| < 1.1$, leaving phase space available for the associated jets (enabling jet of both lower and higher p_T). Finally, the reconstructed Z-boson[13] is required to be back-to-back in the transverse plane with respect to the jet with the highest p_T: $|\Delta\phi(Z, \text{jet})| > 2.6$ rad. Due to the already minimalistic jet subtraction method and analysis used in this paper, the lepton radiation ($l \to l + \gamma$), in the simulation, is switched off[14] in order to simplify the analysis by neglecting corrections for QED final state radiation.

5.2.1 Centrality Selection

For the analysis of pPb collisions, the centrality boundaries are obtained from the generated transverse energy spectrum, which is based on the sum of transverse energy,$\sum E_T$, in the pseudorapidity interval between -4.9 and -3.2 (the Pb-going directions). The $\sum E_T$ distribution obtained from minimum bias events[15] in these collisions is divided into separate ranges of $\sum E_T$ referred as *centrality classes*. The centrality boundaries used in the analysis, starting with percentage of minimum bias events with the largest $\sum E_T$ corresponding to the most central collisions, are 1%, 5%, 10%, 20%, 30%, 40%, 60% and 90%. These boundaries were obtained using the same observable as was used for pPb in the ATLAS analysis [44].

The centrality for the minimum bias PbPb collisions is determined in the same way as for pPb collisions, however the centrality is characterised by the $\sum E_T$ in the both beam directions, $3.2 < |\eta| < 4.9$. The centrality boundaries used in this analysis are 5%, 10%, 20%, 30%, 40%, 50%, 60%, 70% and 80%, based on the [45] ALICE analysis.

5.3 Jet Reconstruction

The jet reconstruction is performed on the record of all particles in each event, excluding[16] the Z^0-candidate's decay products and particles outside the $|\eta| < 3.6$ interval. The cluster-

[12]The production of Z-bosons with a associated parton is a next-to-leading (NLO) Drell-Yan process, given by: $q + \bar{q} \to Z^0 g$ and $q(/\bar{q}) + g \to Z^0 + q(/\bar{q})$).

[13]In this thesis, "reconstructed Z-boson" refers to the reconstructed four-momentum vector of the Z-boson, i.e. sum of four-momentum of the boson's decay products (electron pair).

[14]If the lepton radiation of photon was switched on, it would have resulted into minor smearing of the measurements.

[15]The selection of minimum bias events is preformed in order to minimize the selection bias of the centrality. The reason behind this choice is due to the relatively low transverse energy of the background in pPb collisions, which becomes a problem when studying high-p_T jets. This would have biased events towards jet productions of larger transverse energy in the given η-interval of the centrality selection. Note that this bias remains small in PbPb collisions due to the negligence of the jet energy compared the underlying event energy.

[16]The excluded particles are either outside the detector range or undetectable, and therefore excluded from the analysis. The Z^0-candidate's decay products are excluded since they are included in the other half of the observable.

ing of particles is performed with the anti-k_T sequential recombination algorithm with a radius parameter $R = 0.5$ in the $y - \phi$ space, the rest of the jet-definition parameters were left on the default setting. The anti-k_T algorithm was used to reconstruct jets due to its jet boundary being resilient to soft (low p_T) radiation, which is produced in great abundance in heavy-ion collisions, while flexible towards hard (high p_T) radiation, i.e. hard radiation has great influence on the jet area. If the k_T-algorithm was to be used, we would have observed event-by-event and jet-by-jet fluctuations of the jet area and larger smearing of jet momenta due to UE radiation. The resilience to soft radiation is due to the fact that it tense to cluster soft particles to the hard ones instead of with other soft particles. This leads to accumulation of all soft particles within the given radius parameter R around a hard core, resulting in a conical jet if there are no neighbouring hard particles within a distance of $2R$. These properties are further explained in [46]. The jet reconstruction ends with subtracting the contribution of the UE from the jet. The jet subtraction process is explained in the following section, Section 5.4.2.

5.4 The Underlying Event Analysis and Subtraction

Let's begin by explaining the most general idea used for UE analysis and jet subtraction, then we will introduce a slight modification to this algorithm.

The simplest idea of estimating the contribution from the UE is by finding out the background p_T density (p_T/A) outside of the jet area and then subtracting the contribution from the jet, while assuming constant density[17].

The used method for UE estimation is a jet-based background estimator, which involves taking the median of the p_T/A distribution for the pseudo jets in a given event or region of the event[18], as proposed in [49].

The slightly "modified UE subtraction" involves choosing the region of the event (for the jet-based background estimator) which lies in the same rapidity space as the jet in question y_{jet}, while turning the azimuthal angle towards the direction of the reconstructed Z-boson ϕ_Z (see the results of this selection in section 6.5). This assumes that the p_T density of the UE is constant with azimuthal angle[19]. The reasoning behind the choice of the azimuthal angle is that the region of the jet is occupied by the signal of the jet and the UE. However, the region of the Z-boson's decay products (created from back-to-back hard scattering process) is just occupied by the high p_T dielectron pair and the underlying event.

[17] This is a oversimplification. For example, the energy density has a rapidity dependence[47], which is especially true for pA collisions, which are inherently asymmetric.

[18] As mentioned in the Fastjet manual, this method is largely insensitive to the presence at a handful of hard jets, and avoids any need for introducing a p_T scale to distinguish hard and background jets. The recommended region of resolution parameter R^* with the least bias for UE density determination is $R = 0.4 - 0.6$ [48]. The higher range is preferred for sparse events in order to not underestimate the UE.

[19] This assumption turns out to be false due to anisotropic radial flow, affecting the azimuthal distribution. However, the modified version of the jet subtraction performs its analysis at azimuthal opposite directions, correcting for the elliptic flow (higher order harmonic flow are due to the fluctuations in the initial matter distribution, which are small and neglected in this thesis).

The UE analysis is done by reconstructing pseudo-jets with a resolution parameter R^* [20] inside a circle of radius, referred as "SCR" in this thesis, centred at (y_{jet}, ϕ_Z). The p_T density of the UE, ρ_{UE}, is calculated by summing over the p_T of all constituents of the pseudo-jet and dividing by the area produced in the algorithm, see 5.4.1. Note that the k_T-algorithm used for the UE analysis (the analysis setup is described in section 5.4.2) do not give jets with areas corresponding to a perfect circle. However, the tools needed to do the calculations of p_T densities of the UE in a given region are provided by FastJet. The criteria for the selection of the UE estimate is $|\eta^{\text{jet}}| < 3.6$ and the exclusion of the 2 hardest jets.

5.4.1 Jet Area

An active area is a jet area definition used in FastJet. It is used to measure the susceptibility for a jet to diffuse radiation, which is embodied in the jet area. The ambiguous jet area (jets consists of pointlike particles with no intrinsic area definition) is define by first introducing a uniform distribution in y, ϕ of infinitely soft massless "ghost" particles, the method is called *active area*. Next, the area of a jet is identified as the region of ghosts that are clustered with a given jet. In this thesis, we used the *active area* method in combination with *explicit ghosts* which includes ghosts when the constituents of a jet are requested and also leads to the presence of "pure ghost" jets (and ensures the safest treatment of these jets) , which accounts for the empty region in a events when calculating the UE density median.

5.4.2 Underlying event Analysis Setup

The UE analysis was performed by utilizing the FastJet software package, version 3.3.0.

Each of the generated collisions types (pp, pPb and PbPb) underwent underlying event (UE) subtraction with an event-by-event approach, by estimating the transverse momentum density, $\rho(\eta, \phi)$, with the method explained in the previous section . The UE estimator used here was the jet-based method[21], with the recommended settings (see section 8.1.1 in the FastJet manual [50]): k_t-algorithms with R-value of 0.3[22] and an active area (as standard for jets reconstructed in the ALICE collaboration) with explicit ghosts. The choice of the resolution parameter R, in the UE analysis, was based on the expectancy that high multiplicities would occur in the events, which otherwise would have given rise to fluctuation effects in the underlying event. Note that the leading jet is excluded from the underlying event analysis, as otherwise it would be biased if the p_T in a jet is included in their calculation, which would result in an over-subtraction of the underlying events contribution to the jet's p_T.

[20] In heavy-ion collisions, the radius parameter is kept at low values, in order to minimize the fluctuations caused by contamination of hard particles (as stated and recommended in the Fastjet manual [50]). This is under the assumption that the fluctuation in the UE per event remains small in comparison to the UE density, which can be expected.

[21] The used method was called `fastjet::JetMedianBackgroundEstimator`.

[22] The low R value of < 0.4 is preferred for busy events, as stated in the FastJet manual.

Requirements on Z-bosons candidate (its decay products):
$\lvert\eta^{e^-}\rvert, \lvert\eta^{e^+}\rvert < 1.1$ and $p_T^{e^-}, p_T^{e^+} > 20$ GeV/c
Requirements on jets:
anti-k_T algorithm with $R = 0.5$
the leading jet within $\lvert\eta^{\text{jet}}\rvert < 3.6$ and $\lvert\Delta\phi(Z, \text{jet})\rvert = \lvert\phi^Z - \phi^{\text{jet}}\rvert > 2.6$ is selected
$p_T^{jet} > 30$ GeV/c (after UE subtraction)
UE estimation and subtraction
k_T algorithm with resolution parameter $R^* = 0.3$
Area definition: active area explicit ghost

Table 2: Summary of the requirements at particle level that define the fiducial phase-space region of the measurements.

6 Results

In this chapter, the results of the previously described analysis are presented. The collision events were generated by PYTHIA8, for proton-lead (pPb) collisions at $\sqrt{s_{NN}} = 5.012$ TeV, lead-lead (PbPb) collisions at $\sqrt{s_{NN}} = 2.76$ TeV and compared with proton-proton (pp) collisions with the corresponding collision energy.

In the first two sections, the $\Delta\phi$ and $\Delta\eta$ momentum distributions with respect to high-p_T Z-bosons and leading jets (selected in accordance to the requirements in table 2) are studied for different centralities. Next, measurements of the transverse momentum ratio, $x_{JZ} = p_T^{jet}/p_T^Z$, of Z+jet as a function of centrality are presented. In section 6.4, the jet momentum density profile is measured as a function of $\Delta r = \sqrt{(\Delta\eta)^2 + (\Delta\phi)^2}$ for Z+jet events, in comparison to PbPb and pPb to pp jet shapes up to $\Delta r = 0.5$ and in different intervals of centrality. In the last section, the analysis of the modified UE subtraction, described in 5.4.2, is presented.

The presented measurements in figures 7, 8, 9 and 10 are performed with "(sub)" or without "(UE)" UE subtraction when reconstructing the jets, with the notation given in the line label. The remaining information is arranged accordingly: the centrality class percentile is declared at the top of each sub-plot, most central (left) to most peripheral (right), and the collision energy is presented in the last column. The continuous line represents the pPb/PbPb collisions and the dashed line represents the pp collisions with correspond energy.

At the beginning of each section, an explanation of the graph's general appearance is presented and a comment of our expectations of how the graph would look like[23] will be given. Then we will discuss the differences between the results obtained from the pp collisions and the collisions involving a heavy-ion. An emphasis will be placed on the performance of the jet subtraction in PbPb and pPb collisions using pp collisions as reference.

[23]In ref. [51] one can simulate typical jet observables with different parameters, allowing us to have a sense of how it should look like.

The statistical error have been calculated for each observable. However, the statistical error is not explicitly shown on any of the graphs, partly due to the fact that it is small[24]. Another reason is that the scale of the statistical error is directly proportional to the visual statistical fluctuations, and thus giving a sense of the magnitude of the error.

Let's begin by establishing the pp reference, by comparing the results for each of the observables in pp events with and w/o MPI and UE subtraction. Note that no MPI events contain the "purest" jets (jets without noise),as the major contribution for the UE comes from MPI, while MPI events are the closest to actual events (neglecting leptons radiating photons, pile-up and detector response, etc.). For pseudorapidity, p_T ratio and azimuthal angle correlations, each setting results in a very similar distributions. The jet profile observables shows, however, a more centred jet constituents distribution for no MPI events, which is expected and a sign that our UE subtraction needs a slight modification. There are, however, no/minuscule differences when using UE subtraction. This is probably due to the sparse and low p_T underlying event in pp collisions. In conclusion, we will only use the pp events with MPI and UE subtraction for further uses, as there are no major differences between the pp references.

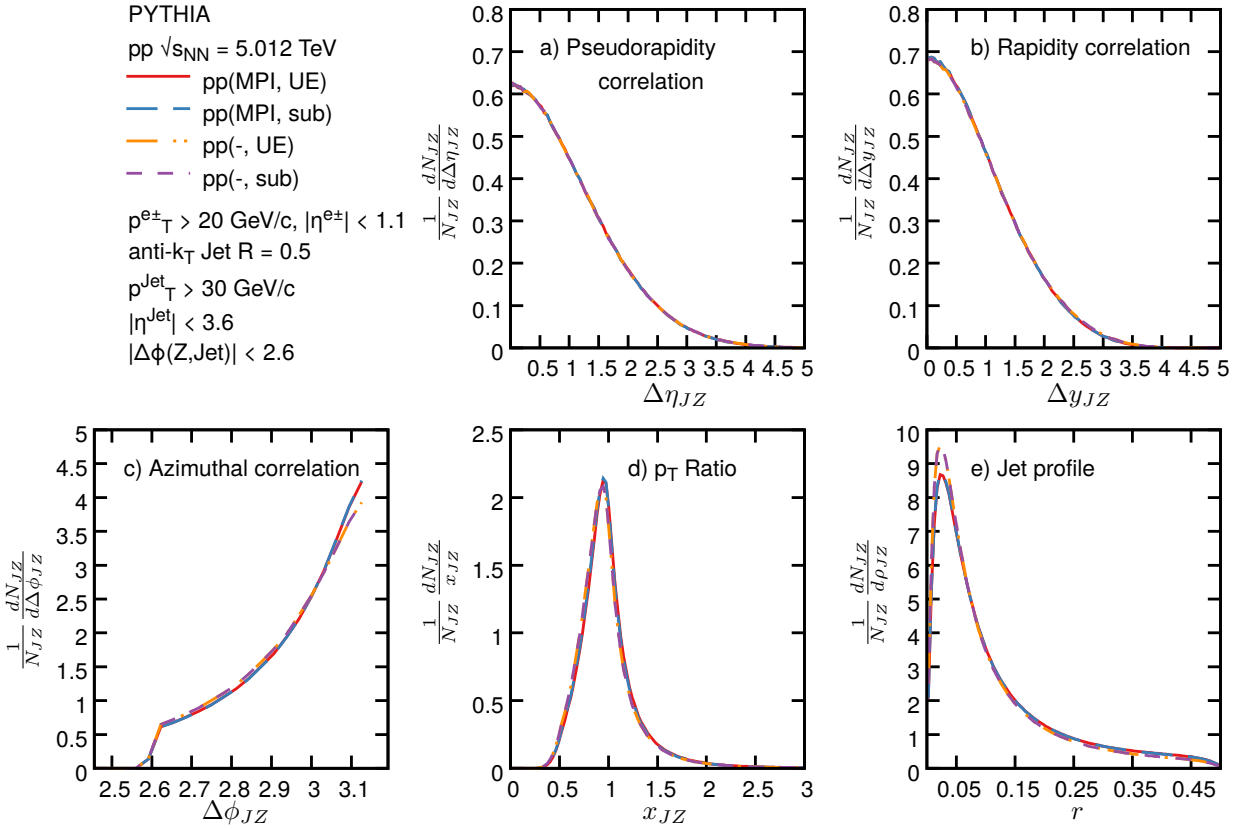

Figure 6: Results of UE subtraction performance in pp collisions for each of the observables, where the setting for MPI were on/off (MPI,-), with and without UE subtraction, are compared.

[24]The given results are of high statistic, just over 10^6 passed events.

6.1 Z-boson+jet azimuthal correlation

The results of the azimuthal difference, $\Delta\phi_{JZ} = |\phi^{Jet} - \phi^{Z}|$[25], between the Z-boson and the selected jet are presented in figure 7. The shapes of the event-normalized differential Z+jet distribution, $(1/N)(dN/d\Delta\phi_{JZ})$, against $\Delta\phi_{JZ}$ are normally used to study the change of the back-to-back alignment of the Z-boson and the parton, as a possible medium effect.

The general features of the graphs are according to our expectations. The expectation is that since the jet is the result of a parton recoil on the opposite away-side of the Z-bosons, $\Delta\phi \approx \pi$, the measured azimuthal angle would then be distributed with a mean at $\Delta\phi \approx \pi$ (the graphs reaches its peak at $\Delta\phi_{JZ} = \pi$) and with a standard deviation that partially dependent on the underlying event. Do note that the measurement contained a $\Delta\phi_{JZ} > 2.6$ cut[26].

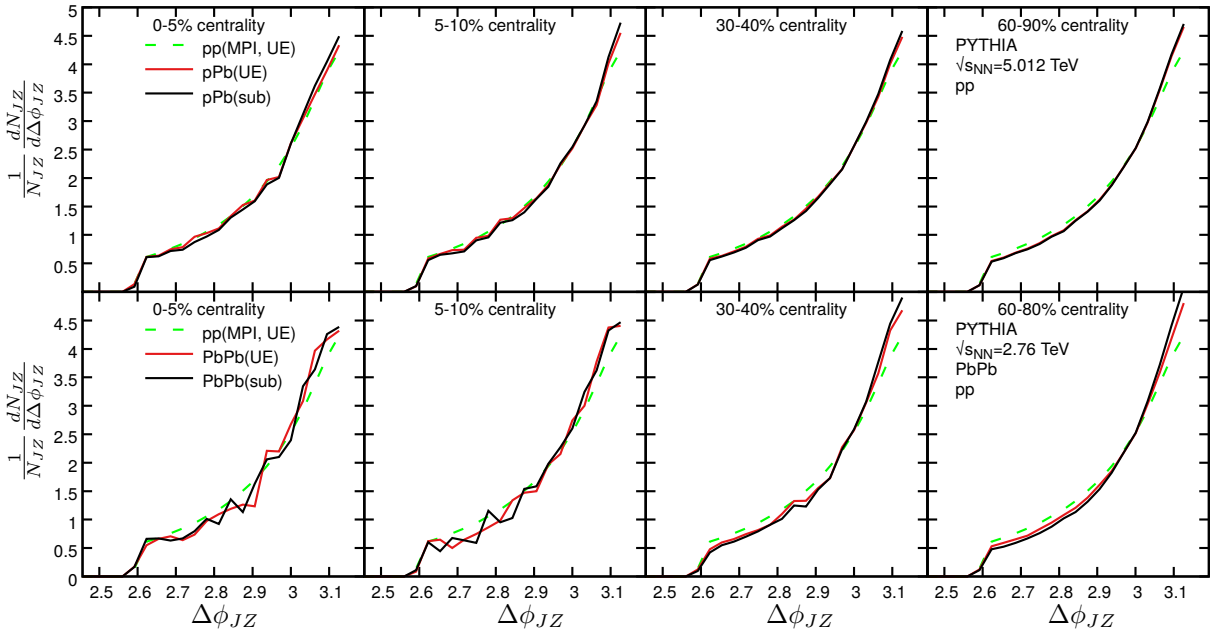

Figure 7: Azimuthal correlation of Z-boson and leading jets of $p_T > 30$ GeV/c and $\Delta\phi_{JZ} > 2.6$ in pPb (top) and PbPb (bottom) simulation, in several centrality ranges, compared to pp without UE subtraction.

The UE subtraction performance for the two most peripheral bins in the PbPb collisions is in good agreement with the pp reference. In general, the UE subtraction results in a bit narrower distribution of $\Delta\phi$, let us conclude that the jet reconstruction (which gives minor differences between events with and without UE subtraction, thus implying that the UE is uniformly distributed in ϕ) and subtraction by estimation of the entire $\eta - \phi$ plane does perform an adequate UE subtraction.

[25]The azimuthal difference can assume values $\Delta\phi \in [0, \pi]$.

[26]The plots go slightly below 2.6 due to the bin resolution.

6.2 Z-boson+jet pseudorapidity correlation

The pseudorapidity correlation between the reconstructed Z-boson and the leading jet is given by $\Delta\eta_{JZ} = |\eta^{Jet} - \eta^{Z}|$, and the results are shown in figure 8. The measurements are as expected, showing a distribution around $\Delta\eta_{JZ} = 0$. These graphs contain similar characteristic differences that are found in the $\Delta\phi_{JZ}$ graphs, concluding that UE subtraction preforms adequately.

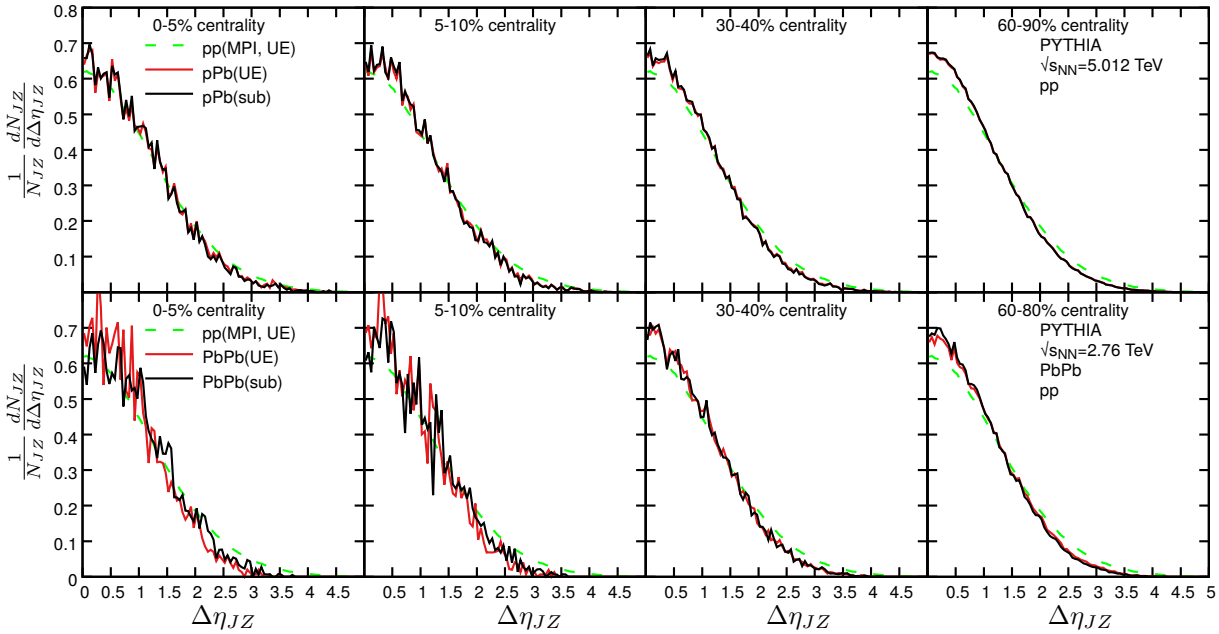

Figure 8: Pseudorapidity correlation of Z-boson and leading jets of $p_T > 30$ GeV/c and $\Delta\phi_{JZ} > 2.6$ in pPb (top) and PbPb (bottom) simulation, in several centrality ranges, compared to pp without UE subtraction.

6.3 Z-boson+jet transverse momentum imbalance

Measurements of the transverse momentum ratio, $x_{JZ} = p_T^{jet}/p_T^Z$, of Z+jet as a function of centrality for pPb and PbPb events are presented in figure 10, as a normalized x_{JZ} distribution. The asymmetry of the x_{JZ} is used to quantify the Z-boson + jet transverse momentum imbalance, under the assumption that the transverse momentum for the Z-boson and the associated initial parton are of the same magnitudes.

On every histogram except for the PbPb events, the peak is found at $x_{JZ} \approx 1$ (implying a small difference between p_T^{jet} and p_T^Z), meaning that there is a good balance between the Z-bosons and the jet. The natural asymmetric distribution is a result of the selection of $p_T^{\text{Jet}} > 30$ GeV/c jets, which imposes a limit on x_{JZ} depending on the choice of p_T^{Jet}. The lower values of x_{JZ} emerges when the p_T^Z distances itself (increasingly) from the p_T^{Jet} cut-off.

The shift of the distribution towards higher x_{JZ} and the change of shape in pPb(UE) (slight modified) and PbPb(UE) (significantly modified, causing the disappearance of the

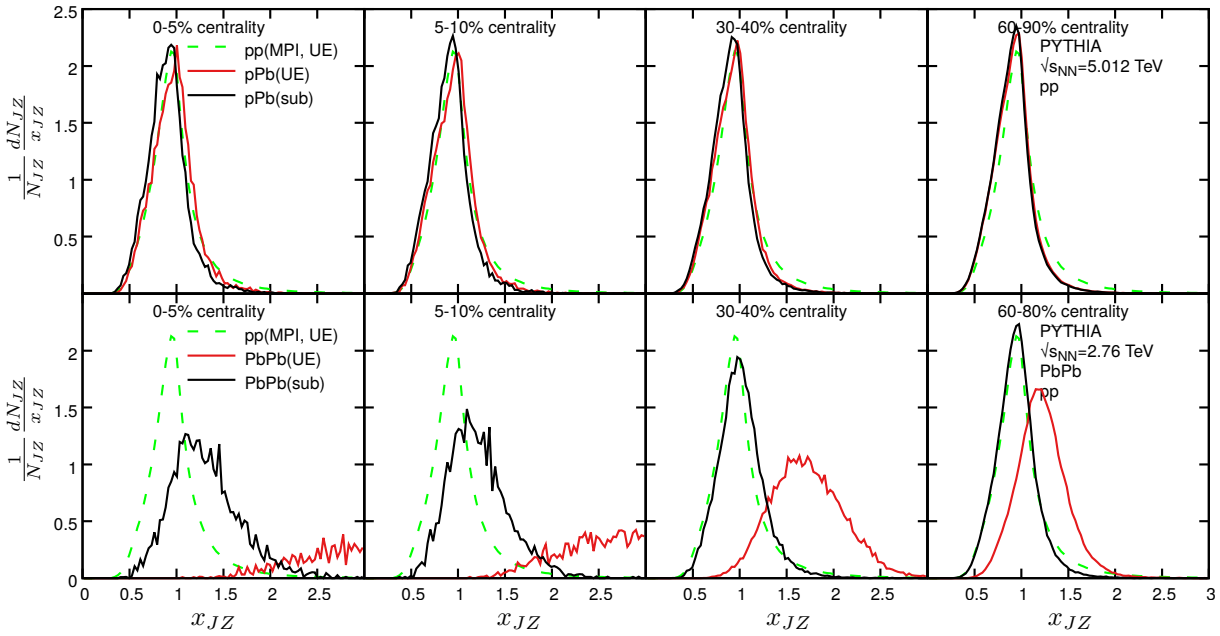

Figure 9: Distribution of x_{JZ} of Z-boson and leading jets of $p_T > 30$ GeV/c and $\Delta\phi_{JZ} > 2.6$ in pPb (top) and PbPb (bottom) simulation, in several centrality ranges, compared to pp without UE subtraction.

peak to right) events, can be attributed to the underlying event. The transverse momentum of the jet receives contribution from the underlying event, resulting in, as can be seen in figure 9, a right shift (the magnitude of the shift is directly proportional to the magnitude of the UE, which in turn depends on the centrality) and an elongated tail to the right. Thus we conclude that both pPb and PbPb collisions have a centrality dependence of x_{JZ}.

In the pPb events and the $60-80\%$ peripheral events in PbPb, the subtraction of UE is performed adequately, as the results are fairly similar to the pp events. In the central collisions of PbPb, the jet subtraction does a significant subtraction of the large p_T contribution of the UE. The way of improving the result is by setting up stricter selection requirements, such as $\Delta\phi$ and higher p_T cut for both the Z-boson and the jet (in order for the anti-k_T algorithm to easier separated the UE from the jet) and reducing the R parameter of the jet finding algorithm (reducing the contribution of the UE).

6.4 The jet profile of the associated jet

The jet profile, or differential jet shape, characterizes the radial distribution of particle transverse momenta[27] inside a jet. The jet profile $\rho_{JZ}(r+\Delta r)$ is defined as:

$$\rho_{JZ}(r+\Delta r) = \frac{1}{\Delta r}\frac{1}{N_{\text{Jets}}}\sum_{\text{Jets}}^{\text{N}}\frac{\sum_{i\in\text{Jet}} p_T(r < r_i < r+\Delta r)}{p_T^{\text{Jet}}} \qquad (6.1)$$

The jet shape $\rho_{JZ}(r+\Delta r)$ is extracted by integrating the jet's p_T distributions in an annulus of the jet cone with a radial width of $\Delta r = 0.005$, where each has an inner radius of r and outer radius of $r+\Delta r$. The p_T distributions are normalized and integrated to unity within the radius $\Delta r < 0.5$.

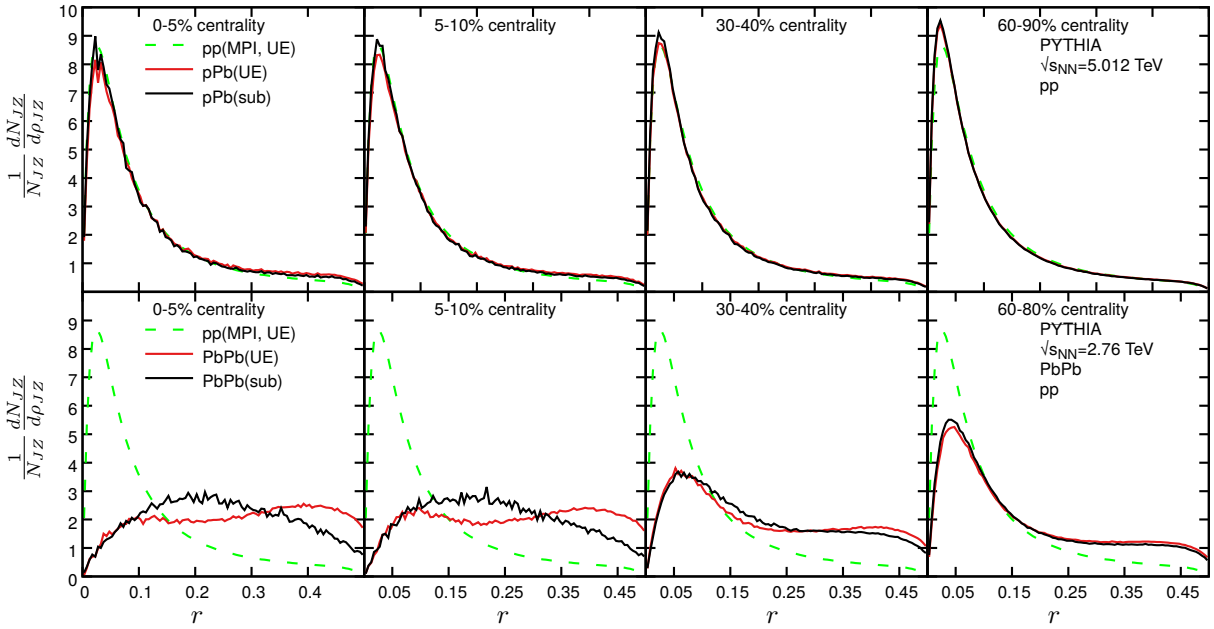

Figure 10: Jet profile of leading jets of $p_T > 30$ GeV/c and $\Delta\phi_{JZ} > 2.6$ in pPb (top) and PbPb (bottom) simulation, in several centrality ranges, compared to pp without UE subtraction.

The shape of the p_T distribution inside a jet in pp and pPb events can be described in the following way: highest density close to the center, progressively lower closer to the edge. The general shape of the distribution is reminiscent of a quark-jet (a jet originating from an initial quark) distribution [52], which has the characteristics: fewer constituents, narrower and harder constituents compared to gluon jets[28]. This agrees with the fact that the Z+jets production is dominated by quark jets [53] for $p_T^{jet} > 30$ GeV/c [54].

[27] The subtraction of the UE is performed by using $(\sum_{i\in\text{Jet}} p_T(r < r_i < r+\Delta r)/p_T^{\text{Jet}} \rightarrow (\sum_{i\in\text{Jet}} p_T(r < r_i < r+\Delta r) - \rho_{\text{UE}}A(r < r_i < r+\Delta r))/p_T^{\text{Subtracted Jet}}$ where ρ_{UE} is the p_T density of the UE and $A(r < r_i < r+\Delta r) = \pi r^2 - \pi(r+\Delta r)^2$ is the area of the annulus.

[28] This property comes from that the gluons are more likely to radiate more gluons than quarks do at the same energy.

The general broadening of the jet structure in central PbPb collisions can be simply explained by the underlying event (centrality dependent) and the geometry of the jet profile. From the jet profile definition, the area ($\propto r^2$) of the bins increases with the distance from the center, giving more room for the UE, consequently increasing the count. Taking a look at the $0-10\%$ centrality plots, we can see that the shape of the "PbPb(UE)" (two local maxima at $r \approx 0.1$ and $r \approx 0.4$) is most likely a result of a normalized superposition of a pp-like jet distribution (which peaks at $r \approx 0.05$) and a large UE contribution (area-dominated, $\propto r^2$, if assumed uniform). Note that the there is a boundary effect, resulting in the edge drop of the jet profile (as seen in each plot), probably due to the way particles are clustered with the anti-k_T algorithm at the boundary. The UE subtraction decreases the tail, but not enough to retain its resemblance of the pp reference. The precise reason for the toroid-like shape of the distribution for PbPb(sub) needs a bit more forethought and study[29], but will most likely result in a similar conclusion.

The underlying event subtraction of the PbPb event performs poorly in comparison to the others observables as the shape of the distribution has no resemblance to the pp reference. A more detailed study on the jet substructure is due, in order to improve the jet subtraction performance. The jet subtraction performance in pPb collisions does an adequate job by narrowing the distribution and thus making it more consistent with the obtained pp results.

6.5 Results of the Modified Jet Subtraction

The differences between the proposed method of subtraction (see section 5.4.2) and the method involving estimating the entire fiducial phase-space (referred to as "UE subtraction") are discussed here. The figures are present in figure 11. The modified method was tested with various radii of the underlying event estimation (SCR) and the radius values of 0.5, 1.0, 1.5, and 2.5, centred at the same ϕ as the Z-boson and the same y as the jet. The results for all the observables, except for p_T ratio, were that the modified subtraction had similar results compared to the UE subtraction. The results of the modified subtraction in p_T balance are however more promising at central collisions ($0-5\%$, including centrality classes $5-30\%$), as can be seen in figure 11, resulting in a more narrow distribution and a significant shift to lower p_T values, placing the peak close to 1. This method shows thus some promising results that can save computing time, by evaluating smaller area for estimation of the underlying event.

7 Discussion

The topic of discussion is the study of jet subtraction performance in heavy-ion collisions without collectivity effects. A major conclusion that can be drawn from this investigation

[29] One can look "behind the scene" and see how well jet direction compares with parton-level direction in order to verify that the jets are the associated ones, but partly contradicted by the nice line up of the azimuthal and pseudorapidity correlation.

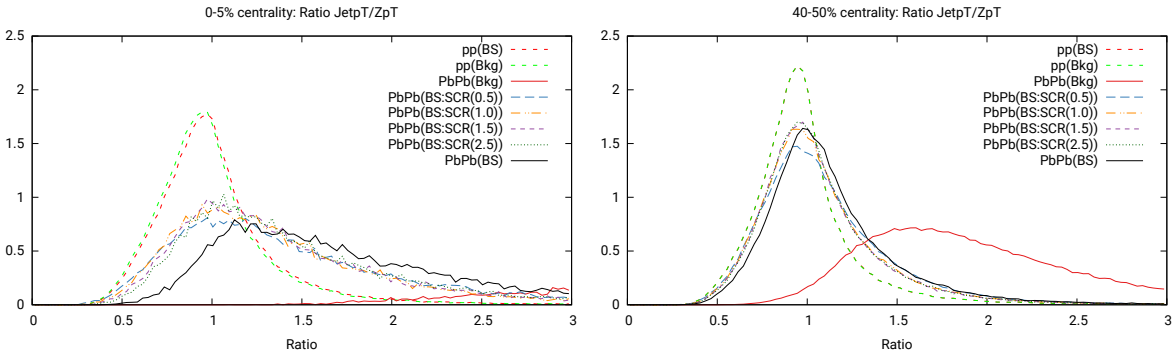

Figure 11: Results of p_T ratio (top row) of Z-boson and leading jets, with the modified underlying event subtraction.

is that the effects of the underlying event are too overwhelming in PbPb events for this type of basic underlying event subtraction.

Besides this, there are several improvements and detailed studies that can be made. Since the majority of the resulting graphs are within reasonable limits of our expectations, concerning the performance of the jet subtraction, there is an argument to be made that the simplistic jet subtraction method used here has some merits. There are, however, some major discrepancies when it comes to the high multiplicity of the underlying PbPb event compared to pp events. We will discuss below several minor modification and detailed studies that may improve the the performance of the jet subtraction.

- One way of improving the performance is with minor modifications to the already existing variables. A type of variable is the requirements or cuts in the Z+jet event selection. This can be improved by applying stricter cuts. For one, a stricter requirement on the jet's azimuthal difference $\Delta\phi_{JZ}$, which would further suppress the contribution of biased-jets from the underlying event, but at the risk of losing interesting information. Another cut modification is a higher p_T-cut for both the Z-boson and the jet, resulting in a better performance from the anti-k_T algorithm on separating the underlying event from the jet.

  Another type of variable is the R parameter. The reduction of the R parameter in the jet finding algorithm would result in a lower contribution from the underlying event.

- In reality, there exists collectivity (collective behaviour) in hadronic collisions, which may affect jet studies. This can manifest itself as an elliptic flow (resulting from an initial spatial anisotropy, mainly due to non-central collisions, i.e. initial elliptic overlap, generating different pressure gradients in the medium, which in turn creates a v_2 azimuthal number density anisotropy). There exists also higher order azimuthal number density anisotropies. An important note is that these are fluctuates on an event-by-event basis and the subtraction of the underlying event must be handled as such, by analysing the p_T density for each event.

- There is also the neglected electromagnetic radiation of the Z-boson's dielectron pair, which would have resulted in a final state radiation effect. This would not improve the jet subtraction, but would improve the realism of the collisions. Other effects that were "swept under the rug" are related to the Angantyr model having uncalibrated parameters, whose adjustment is beyond the scope of this thesis.

- The acceptance rate can be increased, in order to decrease the computational time for the same number of accepted events. This can be done by studying the `PhaseSpace:pTHatMin` (see table 3) parameter in PYTHIA8 in order to maximize the acceptance rate of the p_T cut.

8 Conclusion

Ultra-relativistic heavy-ion collisions are performed at CERN's Relativistic Heavy Ion Collider and the Large Hadron Collider, with the aim of studying the fundamental properties of QCD at extreme conditions of high density and temperature. There are several ways of investigating these properties, one of them being "tomographic" probes, such as jets. However, these jets are accompanied by the overwhelming underlying event of the heavy-ion collisions, making observations of any probe modification problematic, as these changes can't be properly separated from the underlying event.

The method of dealing with the underlying event is called jet subtraction. The basic idea is to estimate the transverse momentum density of the underlying event, while trying to retain the transverse momentum of the jet. The contribution of the transverse momentum from the underlying event is then later subtracted from the jet.

In this work, we have investigated the performance of a very basic jet subtraction method used in heavy-ion collisions. This is done by studying Z-bosons+jet events in pp, pPb and PbPb collisions. The four often used observables are the transverse momentum ratio, azimuthal and pseudorapidity correlations of the Z-bosons and the associated jet, and at last the jet profile or the transverse momentum distribution inside the jet. All observables are studied as a function of collision centrality, with the usage of pp collisions as reference, in order to get a sense of to what degree the jet corrections are dependent on the underlying event.

Our major finding was that the effects of the underlying event are too large for this type of jet subtraction. Our other findings can be summarised as follows

- By the use of the PYTHIA8 and the Angantyr model, we were able to generate the Z+jet events with the full simulated AA underlying event, without the collectivity effects, such as jet quenching and collective flow.

- A modified jet subtraction method is introduced, which performs a local estimation of the underlying event in an area of a circle with a given radius centred at the ϕ of the reconstructed Z-boson and η of the selected jet. This method performs better than the estimation of the entire event plane for the measurements of p_T-ratio, while performing convergently from no effect to the "whole plane estimation" standards.

- The results from the jet subtraction, where the entire underlying event plane was estimated, show that the azimuthal and pseudorapidity correlations were similar to the results obtained from pp collisions. However, the inconsistency without any jet subtraction were minor to begin with.

- The jet subtraction of the observables Δx_{JZ} and the jet profile (which are directly dependent on the magnitude of the measured p_T sum) perform poorly in central collisions, but have some minor promising potential. Reassuringly, the subtraction of pPb and peripheral PbPb (which only tends toward) collisions performs adequately.

  The overall conclusion of the performance of the minimalistic jet subtraction was that the method used in this thesis works reliably (at least in terms of the given model Angantyr) for events densities similar to central pPb collisions. The subtraction of the underlying event in PbPb collisions, however, need to be improved, since there the effects from the underlying event overshadows all other. This will presumably be at a cost of stricter restriction in the selection of events.

References

[1] T. Pierog, I. Karpenko, J. M. Katzy, E. Yatsenko, and K. Werner, "EPOS LHC: Test of collective hadronization with data measured at the CERN Large Hadron Collider," *Phys. Rev.* **C92** no. 3, (2015) 034906, arXiv:1306.0121 [hep-ph].

[2] Z.-W. Lin, C. M. Ko, B.-A. Li, B. Zhang, and S. Pal, "A Multi-phase transport model for relativistic heavy ion collisions," *Phys. Rev.* **C72** (2005) 064901, arXiv:nucl-th/0411110 [nucl-th].

[3] C. Bierlich, G. Gustafson, L. Lönnblad, and H. Shah, "The Angantyr model for Heavy-Ion Collisions in PYTHIA8," arXiv:1806.10820 [hep-ph].

[4] X.-N. Wang and M. Gyulassy, "HIJING: A Monte Carlo model for multiple jet production in p p, p A and A A collisions," *Phys. Rev.* **D44** (1991) 3501–3516.

[5] R. S. Bhalerao and R. V. Gavai, "Heavy Ions at LHC: A Quest for Quark-Gluon Plasma," in *Physics at the Large Hadron Collider*, A. Datta, B. Mukhopadhyaya, A. Raychaudhuri, A. K. Gupta, C. L. Khetrapal, T. Padmanabhan, and M. Vijayan, eds., pp. 105–130. 2009. arXiv:0812.1619 [hep-ph].

[6] **CMS** Collaboration, D. G. d'Enterria *et al.*, "CMS physics technical design report: Addendum on high density QCD with heavy ions," *J. Phys.* **G34** (2007) 2339.

[7] J. D. Bjorken, "Energy Loss of Energetic Partons in Quark - Gluon Plasma: Possible Extinction of High p(t) Jets in Hadron - Hadron Collisions,".

[8] **STAR** Collaboration, C. Adler *et al.*, "Centrality dependence of high p_T hadron suppression in Au+Au collisions at $\sqrt{s_{NN}}$ = 130-GeV," *Phys. Rev. Lett.* **89** (2002) 202301, arXiv:nucl-ex/0206011 [nucl-ex].

[9] **STAR** Collaboration, K. Kauder, "Di-Jet Imbalance Measurements in Central Au+Au Collisions at $\sqrt{s_{NN}} = 200$ GeV from STAR," in *Proceedings, 7th International Conference on Hard and Electromagnetic Probes of High-Energy Nuclear Collisions (Hard Probes 2015): Montréal, Québec, Canada, June 29-July 3, 2015*. 2016. arXiv:1509.08833 [nucl-ex].

[10] **ATLAS** Collaboration, G. Aad *et al.*, "Observation of a Centrality-Dependent Dijet Asymmetry in Lead-Lead Collisions at $\sqrt{s_{NN}} = 2.77$ TeV with the ATLAS Detector at the LHC," *Phys. Rev. Lett.* **105** (2010) 252303, arXiv:1011.6182 [hep-ex].

[11] X.-N. Wang, Z. Huang, and I. Sarcevic, "Jet quenching in the opposite direction of a tagged photon in high-energy heavy ion collisions," *Phys. Rev. Lett.* **77** (1996) 231–234, arXiv:hep-ph/9605213 [hep-ph].

[12] X.-N. Wang and Z. Huang, "Study medium induced parton energy loss in gamma + jet events of high-energy heavy ion collisions," *Phys. Rev.* **C55** (1997) 3047–3061, arXiv:hep-ph/9701227 [hep-ph].

[13] **CMS** Collaboration, S. Chatrchyan *et al.*, "Observation and studies of jet quenching in PbPb collisions at nucleon-nucleon center-of-mass energy = 2.76 TeV," *Phys. Rev.* **C84** (2011) 024906, arXiv:1102.1957 [nucl-ex].

[14] M. Gell-Mann, "The Eightfold Way: A Theory of strong interaction symmetry,".

[15] Y. Ne'eman, "Derivation of strong interactions from a gauge invariance," *Nucl. Phys.* **26** (1961) 222–229. [,34(1961)].

[16] E. V. Shuryak, "Quantum Chromodynamics and the Theory of Superdense Matter," *Phys. Rept.* **61** (1980) 71–158.

[17] S. Bethke, "World Summary of α_s (2012)," arXiv:1210.0325 [hep-ex]. [Nucl. Phys. Proc. Suppl.234,229(2013)].

[18] Z. Fodor and S. D. Katz, "The Phase diagram of quantum chromodynamics," arXiv:0908.3341 [hep-ph].

[19] C. Bierlich, G. Gustafson, and L. Lönnblad, "Collectivity without plasma in hadronic collisions," *Phys. Lett.* **B779** (2018) 58–63, arXiv:1710.09725 [hep-ph].

[20] A. Accardi *et al.*, "Hard probes in heavy ion collisions at the lhc: pdfs, shadowing and pa collisions," in *3rd Workshop on Hard Probes in Heavy Ion Collisions: 3rd Plenary Meeting Geneva, Switzerland, October 7-11, 2002*. 2004. arXiv:hep-ph/0308248 [hep-ph]. https://inspirehep.net/record/642052/files/arXiv:hep-ph_0308248.pdf.

[21] D. G. d'Enterria, "Quark-Gluon Matter," *J. Phys.* **G34** (2007) S53–S82, arXiv:nucl-ex/0611012 [nucl-ex].

[22] K. Yagi, T. Hatsuda, and Y. Miake, "Quark-gluon plasma: From big bang to little bang," *Camb. Monogr. Part. Phys. Nucl. Phys. Cosmol.* **23** (2005) 1–446.

[23] T. Matsui and H. Satz, "J/ψ Suppression by Quark-Gluon Plasma Formation," *Phys. Lett.* **B178** (1986) 416–422.

[24] Particles and Friends., "Evolution of collisions and QGP." https://particlesandfriends.wordpress.com/2016/10/14/evolution-of-collisions-and-qgp/.

[25] T. Alberica, "Participants and spectators at the heavy-ion fireball.," *CERN COURIER* (26 April 2015) .

[26] B. Andersson, G. Gustafson, G. Ingelman, and T. Sjostrand, "Parton Fragmentation and String Dynamics," *Phys. Rept.* **97** (1983) 31–145.

[27] B. Andersson, G. Gustafson, and B. Soderberg, "A General Model for Jet Fragmentation," *Z. Phys.* **C20** (1983) 317.

[28] T. Sjöstrand, "The lund model and some extensions." Workshop on collective effects in small collisions systems, cern, 15 june 2017, 2017.

[29] C. Buttar *et al.*, "Standard Model Handles and Candles Working Group: Tools and Jets Summary Report," in *Physics at TeV colliders, La physique du TeV aux collisionneurs, Les Houches 2007 : 11-29 June 2007*, pp. 121–214. 2008. arXiv:0803.0678 [hep-ph]. https://inspirehep.net/record/780755/files/arXiv:0803.0678.pdf.

[30] L. A. Cruz, *Using MAX/MIN Transverse Regions to Study the Underlying Event in Run 2 at the Tevatron.* PhD thesis, Florida U., 2005. http://wwwlib.umi.com/dissertations/fullcit?p3188071.

[31] **GEANT4** Collaboration, S. Agostinelli *et al.*, "GEANT4: A Simulation toolkit," *Nucl. Instrum. Meth.* **A506** (2003) 250–303.

[32] B. Andersson, G. Gustafson, and B. Nilsson-Almqvist, "A Model for Low p(t) Hadronic Reactions, with Generalizations to Hadron - Nucleus and Nucleus-Nucleus Collisions," *Nucl. Phys.* **B281** (1987) 289–309.

[33] C. Bierlich, G. Gustafson, and L. Lönnblad, "Diffractive and non-diffractive wounded nucleons and final states in pA collisions," *JHEP* **10** (2016) 139, arXiv:1607.04434 [hep-ph].

[34] C. Bierlich, *Rope Hadronization, Geometry and Particle Production in pp and pA Collisions*. PhD thesis, Lund University, 2016.

[35] M. Alvioli and M. Strikman, "Color fluctuation effects in proton-nucleus collisions," *Phys. Lett.* **B722** (2013) 347–354, arXiv:1301.0728 [hep-ph].

[36] C. Bierlich, G. Gustafson, and L. Lönnblad, "A shoving model for collectivity in hadronic collisions," arXiv:1612.05132 [hep-ph].

[37] **ALICE** Collaboration, M. Estienne, "Jet reconstruction in heavy ion collisions: Emphasis on Underlying Event background subtraction," in *Proceedings, 1st International Workshop on Multiple Partonic Interactions at the LHC (MPI08): Perugia, Italy, October 27-31, 2008*, pp. 323–332. 2009. arXiv:0910.2482 [nucl-ex].

[38] **ALICE** Collaboration, J. Adam *et al.*, "Enhanced production of multi-strange hadrons in high-multiplicity proton-proton collisions," *Nature Phys.* **13** (2017) 535–539, arXiv:1606.07424 [nucl-ex].

[39] C. Bierlich and J. R. Christiansen, "Effects of color reconnection on hadron flavor observables," *Phys. Rev.* **D92** no. 9, (2015) 094010, arXiv:1507.02091 [hep-ph].

[40] C. Bierlich, "Rope Hadronization and Strange Particle Production," *EPJ Web Conf.* **171** (2018) 14003, arXiv:1710.04464 [nucl-th].

[41] C. Bierlich, G. Gustafson, L. Lönnblad, and A. Tarasov, "Effects of Overlapping Strings in pp Collisions," *JHEP* **03** (2015) 148, arXiv:1412.6259 [hep-ph].

[42] C. Bierlich, G. Gustafson, and L. Lönnblad, "Collectivity without plasma in hadronic collisions," *Phys. Lett.* **B779** (2018) 58–63, arXiv:1710.09725 [hep-ph].

[43] A. Festanti, *Measurement of the* D^0 *meson production in Pb-Pb and p-Pb collisions with the ALICE experiment at the LHC*. PhD thesis, Padua U., New York, 2015-02-02.

[44] **ATLAS** Collaboration, G. Aad *et al.*, "Measurement of the centrality dependence of the charged-particle pseudorapidity distribution in proton–lead collisions at $\sqrt{s_{\mathrm{NN}}} = 5.02$ TeV with the ATLAS detector," *Eur. Phys. J.* **C76** no. 4, (2016) 199, arXiv:1508.00848 [hep-ex].

[45] **ALICE** Collaboration, K. Aamodt *et al.*, "Centrality dependence of the charged-particle multiplicity density at mid-rapidity in Pb-Pb collisions at $\sqrt{s_{NN}} = 2.76$ TeV," *Phys. Rev. Lett.* **106** (2011) 032301, arXiv:1012.1657 [nucl-ex].

[46] M. Cacciari, G. P. Salam, and G. Soyez, "The Anti-k(t) jet clustering algorithm," *JHEP* **04** (2008) 063, arXiv:0802.1189 [hep-ph].

[47] J. L. Albacete, "Particle multiplicities in Lead-Lead collisions at the LHC from non-linear evolution with running coupling," *Phys. Rev. Lett.* **99** (2007) 262301, arXiv:0707.2545 [hep-ph].

[48] M. Cacciari, G. P. Salam, and S. Sapeta, "On the characterisation of the underlying event," *JHEP* **04** (2010) 065, arXiv:0912.4926 [hep-ph].

[49] M. Cacciari and G. P. Salam, "Pileup subtraction using jet areas," *Phys. Lett.* **B659** (2008) 119–126, arXiv:0707.1378 [hep-ph].

[50] M. Cacciari, G. P. Salam, and G. Soyez, "FastJet User Manual," *Eur. Phys. J.* **C72** (2012) 1896, arXiv:1111.6097 [hep-ph].

[51] J. Gallicchio and M. D. Schwartz, "Quark and Gluon Tagging at the LHC," *Phys. Rev. Lett.* **107** (2011) 172001, arXiv:1106.3076 [hep-ph].

[52] F. Fabbri, "Studies of quark and gluon jet properties at lep," *Nuclear Physics B - Proceedings Supplements* **71** no. 1, (1999) 180 – 186. http://www.sciencedirect.com/science/article/pii/S0920563298003405. Multiparticle dynamics 1997.

[53] **CMS** Collaboration, A. M. Sirunyan *et al.*, "Study of Jet Quenching with $Z+$jet Correlations in Pb-Pb and pp Collisions at $\sqrt{s}_{NN} = 5.02$ TeV," *Phys. Rev. Lett.* **119** no. 8, (2017) 082301, arXiv:1702.01060 [nucl-ex].

[54] R. B. Neufeld, I. Vitev, and B. W. Zhang, "The Physics of Z^0/γ^*-tagged jets at the LHC," *Phys. Rev.* **C83** (2011) 034902, arXiv:1006.2389 [hep-ph].

[55] T. Sjöstrand, "PYTHIA online HTML manual." http://home.thep.lu.se/~torbjorn/pythia82html/Welcome.html, 2017.

A Summary of Event Setup in PYTHIA

Parameter (Common):	**Short Description:**
"Random:setSeed = on"	Indicates that a user-set seed will be used.
"Random:seed = " + SomeRandomValue	The seed to be used.
"WeakBosonAndParton:qqbar2gmZg = on"	Parton scattering: $q\bar{q} \to \gamma^*/Z^0 g$
"WeakBosonAndParton:qg2gmZq = on"	Parton scattering: $qg \to \gamma^*/Z^0 q$
"PhaseSpace:pTHatMin = 20."	The minimum invariant p_T cut in $2 \to 2$ hard-process.
"WeakZ0:gmZmode = 2"	Only pure Z^0 contribution.
"23:onMode = off"	No decay channels for Z^0.
"23:onIfAny = 11 -11"	Z^0 decay only to $e\bar{e}$.
"PartonLevel:MPI = on"	Enable Multiparton Interactions
"TimeShower:QEDshowerByL : off"	Prevent leptons to radiate photons.
Parameter (Heavy-ion collisions):	**Short Description:**
"HeavyIon:SigFitErr = " "0.02,0.02,0.1,0.05,0.05,0.0,0.1,0.0" "HeavyIon:SigFitDefPar = " "17.24,2.15,0.33,0.0,0.0,0.0,0.0,0.0"	Initialize the Angantyr model to fit the total and semi-inclusive cross sections in Pythia within some tolerance. Suitable for $\sqrt{S_{NN}} = 5$ TeV
"HeavyIon:SigFitNGen = 20"	A simple genetic algorithm is run for 20 generations to fit the parameters.

Table 3: Summary of the parameters used for the event set-up run in PYTHIA. Note that this list doesn't contain type, energy or frame-type of the beams. Documentation for these parameters can be found at [55]